

# A covalently cross-linked hyaluronic acid/bacterial cellulose composite hydrogel for potential biological applications

Shuo Tang<sup>a,b,1</sup>, Kai Chi<sup>b,1</sup>, Hui Xu<sup>c</sup>, Qiang Yong<sup>a</sup>, Jian Yang<sup>c</sup>, Jeffrey M. Catchmark<sup>b,\*</sup>

<sup>a</sup> Jiangsu Co-Innovation Center of Efficient Processing and Utilization of Forest Resources, College of Chemical Engineering, Nanjing Forestry University, Nanjing, 210037, People's Republic of China

<sup>b</sup> Department of Agricultural and Biological Engineering, The Pennsylvania State University, University Park, PA, 16802, USA

<sup>c</sup> Department of Biomedical Engineering, Materials Research Institute, The Huck Institutes of the Life Sciences, The Pennsylvania State University, University Park, PA, 16802, USA

## ARTICLE INFO

### Keywords:

Bacterial cellulose  
Hyaluronic acid  
Cross-linked hydrogel  
BDDE  
Biocomposite  
Biocompatibility

## ABSTRACT

Bacterial cellulose (BC) is a good material candidate for wound dressing because of its fine 3-D network structure, high mechanical strength and water holding capability, and good biocompatibility. In this study, a composite hydrogel was prepared by using 1,4-butanediol diglycidyl ether (BDDE) to cross-link BC and hyaluronic acid (HA). Cross-linked BC/HA composites exhibited a denser and smoother surface. This dense morphology improved water retention capability and dimensional stability. BDDE cross-linked BC/HA composite with 2% HA and 1% BDDE showed better overall properties, including water stability (12.7 % water solubility), mechanical properties (tensile strength: ~ 0.61 MPa and Young's modulus: ~1.62 MPa) and thermal stability (maximum degradation temperature: 360 °C), as compared to BC/HA without crosslinking. In addition, cell toxicity assays and morphology indicated the BDDE cross-linked BC/HA composite significantly promoted cell proliferation and adhesion. This chemically cross-linked BC/HA composite may have many new biomedical applications in wound care.

## 1. Introduction

Cellulosic materials have been widely studied and used because of their good renewability, availability, biodegradability, and biocompatibility (Dong et al., 2020). Bacterial cellulose (BC), an exopolysaccharide biosynthesized by certain bacteria (such as *Gluconacetobacter hansenii*, *Rhizobium* and *Rhodobacter*), has widespread use in biomedical applications such as artificial skin, wound dressings, artificial vessels, and scaffolds for tissue engineering due to its high crystallinity, water holding capacity (up to 99 %), ultrafine network structure, robust mechanical properties, and excellent biocompatibility (Carvalho, Guedes, Sousa, Freire, & Santos, 2019; W. K. Czaja, Young, Kaweck, & Brown, 2007; Shah, Ul-Islam, Khattak, & Park, 2013). However, without further modification or functionalization, some inherent disadvantages, such as low activity, difficulties in bioabsorption, and restricted cell adhesion, have limited its wider application in medicine (Chiaoprakobkij, Sanchavanakit, Subbalekha, Pavasant, & Phisalaphong, 2011; Wang, Wan, Luo, Gao, & Huang, 2012).

One widely adopted strategy is to prepare BC-based composite materials that could overcome the aforementioned shortcomings and achieve the synergetic effect between BC and other components. Various multifunctional BC-based composites have been developed, including BC/hemicelluloses (Chi & Catchmark, 2017), BC/hyaluronic acid (de Oliveira et al., 2017; Li, Qing, Zhou, & Yang, 2014), BC/chitosan (Lin, Lien, Yeh, Yu, & Hsu, 2013), BC/gelatin (Treesuppharat, Rojanapanthu, Siangsanoh, Manuspiya, & Ummartyotin, 2017), BC/silk sericin (Lamboni, Li, Liu, & Yang, 2016) and BC/alginate (Chiaoprakobkij et al., 2011). These physical compounding or chemical crosslinking approaches have benefited the resulting BC-based composites in terms of biocompatibility, cell attachment, and fibroblast growth that open up new opportunities in applications such as artificial blood vessels, wound dressing, and tissue regeneration.

Hyaluronic acid (HA) is a high-molecular weight, linear polysaccharide, composed of repeating disaccharide units of  $\beta$ -1,4-D-glucuronic acid (GlcUA) and  $\beta$ -1,3-N-acetyl-D-glucosamine (GlcNAc) linked alternately (Necas, Bartosikova, Brauner, & Kolar, 2008; Weissmann &

\* Corresponding author at: 226 Agricultural Engineering Building, Shortlidge Road, University Park, PA, 16802, USA.

E-mail address: [jmc102@psu.edu](mailto:jmc102@psu.edu) (J.M. Catchmark).

<sup>1</sup> S. Tang and K. Chi contributed equally to this work.

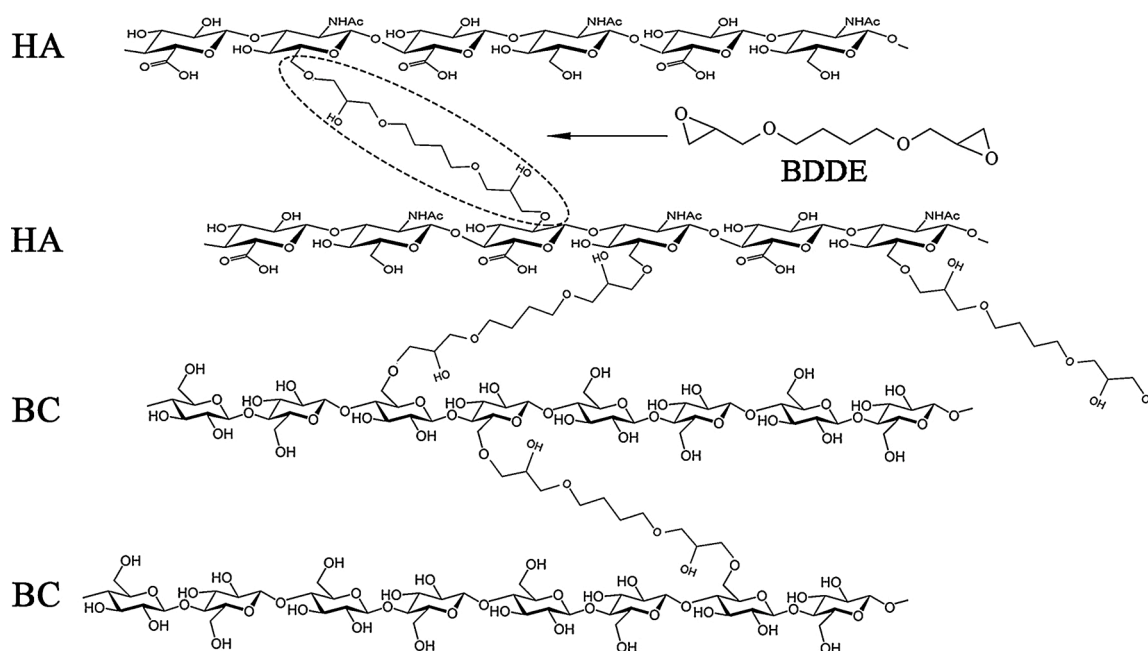


Fig. 1. Schematic representation of the proposed BDDE cross-linked BC/HA composite network.

Meyer, 1954). HA, as a major extracellular component, plays a critical role in several phases of the skin wound repair process. Studies have shown that HA enhances the proliferation and differentiation of endothelial cells and facilitates cell migration, angiogenesis and inflammation regulation during wound healing (Cen, Neoh, Li, & Kang, 2004; Prosdocimi & Bevilacqua, 2012). However, HA has poor mechanical properties and suffers from rapid degradation and clearance *in vivo*, limiting its application in its natural state (Jeon et al., 2007; Pitarresi, Palumbo, Tripodo, Cavallaro, & Giammona, 2007). These unsatisfactory shortcomings can be compensated for by implementing a chemical crosslinking approach. A frequently used method today for cross-linking HA is the reaction with 1,4-butanediol diglycidyl ether (BDDE) under alkaline conditions to yield a stable covalent ether linkage between HA and the cross-linker (De Boule et al., 2013). For example, HA has been immobilized on polyethylene terephthalate (PET) surface via BDDE to enhance blood compatibility and endothelialization (Ramachandran, Chakraborty, Kannan, Dixit, & Muthuvijayan, 2019). In previous studies, BC/HA composites have been prepared by simple soaking, which is essentially a physical compounding approach, and have shown good biocompatibility (Jia et al., 2015; Li et al., 2015). Similarly, due to the similar saccharide structure and abundant hydroxyl groups, such BDDE-induced cross-linking can also occur between BC and HA. HA can either be associated on the surface or imbedded within the network structure of BC by BDDE-induced cross-linking. To the best of our knowledge, the chemical crosslinking approach has yet to be reported in the BC/HA system. In other BC/polysaccharide systems, it has been demonstrated that excellent mechanical properties of composite hydrogels can be achieved by chemical cross-linking. For example, double-network (DN) hydrogels with high mechanical strength have been synthesized using BC and gelatin by EDC crosslinking (Nakayama et al., 2004). Glutaraldehyde was employed as a cross-linking agent to form a hydrogel by copolymerization between BC and gelatin (Treesuppharat et al., 2017). BC offers a large surface area and low bulk density, as well as hydrophilicity. HA can penetrate into BC and cross-link. The existence of BC in HA-based hydrogels can offer enhancement with regard to their tensile strength and dimensional stability when employed under externally applied forces. The combination of BC and HA is expected to improve BC as a biomaterial while increasing the duration of HA in the body or wound site.

In the present study, a chemical crosslinking was established in the

BC/HA system by using BDDE for the first time. The major goal of this study is to obtain better-performing BC-based materials for biomedical applications. Different HA concentrations and BDDE incorporation levels were studied to optimize the properties of the resulting BC/HA composite hydrogel. The morphological, structural, mechanical, and thermal response variations of BC/HA composites were analyzed. Improvement in compression modulus and water retention capacity, and tailored porosity have been observed. In addition, the cross-linked BC/HA composite hydrogel facilitated the growth of mouse fibroblast cells, demonstrating their low toxicity.

## 2. Materials and methods

### 2.1. Materials and reagents

The bacterial strain *Gluconacetobacter hansenii* (*G. hansenii*, ATCC 53582) was obtained from the bioresource center of American Type Culture Collection. Hyaluronic acid sodium salt (HA; Mw  $1.3 \times 10^6$  Da) was purchased from Shandong Freda Biopharm Co., Ltd. (Jinan, China). BDDE was purchased from Sigma Aldrich (MN, USA). All other employed reagents were A.C.S. grade and used without modification.

### 2.2. Production of BC pellicles

BC was biosynthesized by *G. hansenii* by growing the bacteria in a Hestrin and Schramm (HS) medium containing 5 g/L yeast extract, 20 g/L glucose, 5 g/L peptone, 1.15 g/L citric acid, and 2.7 g/L  $\text{Na}_2\text{HPO}_4$  as reported previously (Chi & Catchmark, 2017; Liu & Catchmark, 2019a). Briefly, before incubation, the pH was adjusted to 5.0 and the medium was sterilized for 20 min at 121 °C. A 5% pre-culture of *G. xylinum* was inoculated into the liquid HS-medium and incubated statically in rectangular containers (20 cm × 15 cm × 5 cm) or 96-well plates for production of BC pellicles. After 4-day cultivation, BC pellicles were formed at the air-medium interface, then harvested and purified in 0.1 M NaOH aqueous solution at 80 °C overnight to remove any live cells and cell debris followed by rinsing with ultra-pure water (Millipore Milli-Q UF Plus) until a pH of 7 was achieved. The washed and sterilized BC pellicles were stored in ultra-pure water at 4 °C for further use.

### 2.3. Preparation of BC/HA composites

BC/HA composites were prepared by solution impregnation. BC pellicles were added (to a concentration of 20 % (w/w)) to a HA solution containing 0.1 M NaOH at a concentration of either 0.5, 1 or 2 % (w/v) for 24 h at room temperature. Then, the composite was immersed in BDDE solution containing 0.1 M NaOH for 12 h at 30 °C to allow chemical crosslinking to occur. The BDDE concentration was varied from 0.1 to 1% (w/v). After the reaction, the samples were dipped into 0.1 M HCl to change the pH rapidly and then the samples were washed with ultra-pure water to remove the residual chemicals. The samples were named as BC/HA<sub>x-y</sub>, where x and y are the concentration (wt %) of HA and BDDE, respectively. A schematic illustration of BC-HA interaction is proposed in Fig. 1. After incorporating HA in a physically mixed BC/HA system, covalent ether linkage could be formed among adjacent HA-HA, BC-HA, BC-BC polymer chains. In addition, other interactions such as hydrogen bonding and macromolecule entanglements are speculated to occur due to abundant surface hydroxyl groups and interconnected BC-HA network structure.

### 2.4. Characterization of BC and BC/HA composites

#### 2.4.1. Attenuated total reflectance Fourier transform infrared spectroscopy (ATR-FTIR)

Fourier-transform infrared spectra (FT-IR) were recorded at room temperature in adsorption mode from an accumulation of 32 scans at 4 cm<sup>-1</sup> over the wavenumber range of 4000–400 cm<sup>-1</sup>, using a VERTEX 70 V (Bruker, Germany) spectrometer with an attenuated total reflection (ATR) diamond sensor.

#### 2.4.2. Field emission scanning electron microscopy (FE-SEM) analysis

The surface morphology and microstructure of BC and BC/HA composites were characterized by field emission scanning electron microscopy (Nova NanoSEM, USA) with an accelerating potential of 5.0 kV. All the freeze-dried samples were sputter-coated with a thin layer of iridium (~5 nm) for 30 s before imaging.

#### 2.4.3. X-ray diffraction (XRD)

The crystallinity index (CrI) and crystallite dimensions of BC and BC/HA composites were assessed by a PANalytical Empyrean diffractometer (PANalytical, USA) with Cu K $\alpha$  radiation generated at 45 kV and 40 mA. The lyophilized BC and BC/HA composites were pressed into flat pieces and mounted onto a quartz sample holder. The data was recorded in reflection mode at a rate of 2° min<sup>-1</sup> from 5°–40° with a step size of 0.026°. The CrI was calculated by the peak deconvolution method according to our previous study (Chi & Catchmark, 2017). The crystallite sizes were calculated from the three major lattice planes using the Scherrer equation:

$$D_{hkl} = \frac{k\lambda}{B_{hkl} \cdot \cos\theta}$$

where k is the Scherrer constant ( $k = 0.9$ ),  $\lambda$  is the wavelength of incident X-rays ( $\lambda = 0.15418$  nm),  $B_{hkl}$  is the full-width at half-maximum of the reflection  $hkl$  in radians, and  $\theta$  is the Bragg angle.

#### 2.4.4. Thermogravimetric analysis (TGA)

The thermal stability of BC and BC/HA composites was analyzed by a thermo-gravimetric analyzer TGA Q50 (TA Instruments Inc., New Castle, USA). Approximately 5 mg of lyophilized sample was loaded into an aluminum pan and heated from 35–600 °C at a heating rate of 20 °C min<sup>-1</sup> under nitrogen atmosphere (60 mL/min). The maximum thermal degradation temperature ( $T_{max}$ ) was determined from the peak of the derivative thermogravimetric (DTG) curve. All the experiments were performed at least in duplicate under these experimental conditions.

### 2.4.5. Mechanical tests

A tensile-compressive tester (Instron model 3345) was used to measure the mechanical properties of BC and BC/HA wet pellicles. For the compression tests, the samples were cut into a 10 mm wide square and compressed perpendicular to the BC layers by two parallel metal plates at a strain rate of 1 mm/min. Tests were performed at room temperature. Stress ( $\sigma$ ) was calculated by  $F/A$  where  $F$  is loading force in Newton (N) and  $A$  is the cross-section area measured as width  $\times$  thickness of sample. Strain ( $\epsilon$ ) was calculated by  $\Delta L/L_0$  where  $L_0$  is the initial length and  $\Delta L$  is exerted compression from the starting point. Modulus under compression was calculated by stress/strain in the linear region. For the tensile tests, the samples were cut into 40  $\times$  4 mm (length  $\times$  width) plates and the thickness was measured prior to loading the samples for testing. All the samples were tested at a stretching speed of 2 mm/min. The tensile strength (MPa), Young's modulus (MPa) and strain at break (%) were recorded. Stress and strain between  $\epsilon = 15$  % and 25 % were used to calculate the initial elastic modulus (E). For each material, the results reported are the average values for  $n = 4$  measurements.

### 2.5. Weight loss experiments

The water on the surface of BC and BC/HA composites was quickly removed with filter paper, then samples were placed on aluminum pans and weighed. The wet samples were subsequently dried at 25 °C until their weight became stable. The percent weight loss of the films was determined using  $w = (w_0 - w_t)/w_0$ , where  $w_0$  is the initial weight and  $w_t$  is the weight of wet pellicles at different time, respectively.

### 2.6. Water swelling experiments

For the water swelling test, samples were cut into a 10 mm wide square and compressed perpendicular to the BC layers by two parallel metal plates with a force of 200 N. Then compressed samples were immersed in deionized water for 24 h to allow them to recover naturally. The percentage of recovery is determined using:  $R = (t_0 - t_t)/t_0 \times 100$  %, where  $t_0$  is the initial thickness and  $t_t$  is the thickness of samples after compression or recovery, respectively.

### 2.7. Water solubility experiments

The stability of samples in an aqueous environment was determined by the weight method. The gel samples of BC, BC/HA<sub>2-0</sub> and BC/HA<sub>2-1</sub> measuring at 2  $\times$  2 cm after freeze-drying were obtained by the method described herein. Each sample was weighed to determine the initial dry weight ( $W_0$ ) and was placed in a glass beaker containing 100 mL of distilled water, and gently shaken at 37 °C for 24 h. Then, the sample in distilled water was dried at 105 °C for 6 h until a constant weight was recorded to determine the final dry weight ( $W_f$ ). The cumulative percentage release was calculated as follows: Cumulative percentage release (%) =  $(W_0 - W_f)/W_0 \times 100$  %.

### 2.8. Biocompatibility assessment

For cell proliferation assays, mouse fibroblast (L929) cells were thawed and grown as monolayer in the high-glucose Dulbecco's modified Eagle's medium (DMEM) containing 10 % fetal bovine serum (FBS) and 1% Pen-Strep, and incubated in a humidified air with 5% CO<sub>2</sub> at 37 °C. Cells should be passaged at least 3 times before using them in the biocompatible application. L929 cells were cultured in 96-well plates (1  $\times$  10<sup>4</sup> cells per well) on BC, BC-HA composite films for 1 day, 3 days, and 5 days. Finally, 10  $\mu$ L of CCK-8 reagent was added to each well and further incubation took place over 1 h at 37 °C & 5% CO<sub>2</sub>. After incubation, the CCK-8 solution in each well was transferred into a new 96-well plate for plate reader (iMark (168–1130), Bio-Rad, USA) reading at 450 nm.

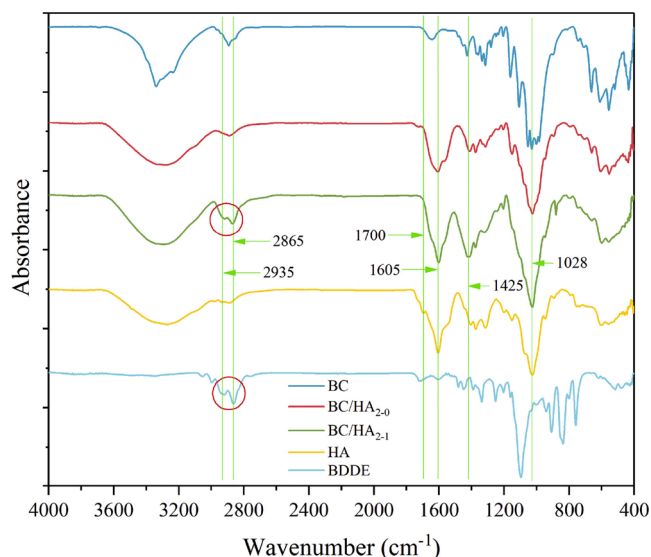


Fig. 2. ATR-FTIR spectra of BC, HA, BDDE and BC/HA composites.

A fluorescence microscope was used to record cell fluorescence images. The live/death of cells on the surface of the BC/HA composite is detected by the dual fluorescent Calcein AM/Ethidium homodimer-1 analysis reagent. After cell cultivation for 5 days, 200  $\mu\text{L}$  of fluorescent reagent was added into each well, followed by 20 min incubation at 37  $^{\circ}\text{C}$  in a 5%  $\text{CO}_2$  incubator. The cells were visualized under a Nikon Eclipse fluorescent microscope (Eclipse Ti2, Nikon, Japan).

Cells adhesion on scaffolds for 5 days was imaged using SEM. BC/HA composite substrates containing cells were washed with Dulbecco's phosphate buffered saline (DPBS) twice and fixed with 2.5 % formaldehyde overnight at 4  $^{\circ}\text{C}$ . Next, a series of gradient concentrations of ethanol containing 25%, 50%, 70%, 85%, 95%, and 100% ethanol (each for 10 min) was applied one by one to dehydrate samples in a biological hood. Dried samples were coated with gold and then observed by SEM (Zeiss, Oberkochen, Germany) operating at 3 Kv.

## 2.9. Statistical analysis

All experiments were carried out at least in triplicate, and results were expressed as mean  $\pm$  SD. Statistical analysis was performed using a student's t-test and SPSS 20 software. The difference with  $P < 0.05$  was considered statistically significant.

## 3. Results and discussion

### 3.1. Characterization of BC and BC/HA composites

#### 3.1.1. ATR-FTIR analysis

The ATR-FTIR spectra acquired from the various samples and BDDE are shown superimposed in Fig. 2. Typical polysaccharide  $-\text{OH}$  signals can be identified at the region between the 3000  $\text{cm}^{-1}$ –3700  $\text{cm}^{-1}$ . However, the peak shape of the original BC is significantly different from that of the HA-containing samples, which may be due to the  $-\text{NH}$  vibration in HA also occurring in this region. The peak at 1605  $\text{cm}^{-1}$  and 1425  $\text{cm}^{-1}$  were attributed to the antisymmetric stretching vibration and symmetric stretching vibration of  $-\text{COO}-$ . According to reports, the  $-\text{CN}-$  of the amide II group and the  $-\text{COO}-$  have an overlapping vibration region at around 1425  $\text{cm}^{-1}$  (Ramachandran et al., 2019). None of these characteristic peaks existed in the original BC, and the peak at 1028  $\text{cm}^{-1}$  in the BC/HA composite is very similar to HA, indicating that HA was successfully incorporated into the BC. For BC/HA<sub>2-1</sub>, two new peaks representing symmetrical and asymmetrical stretching vibration of  $\text{CH}_2$  appeared at 2865  $\text{cm}^{-1}$  and 2935  $\text{cm}^{-1}$ , which are mainly due to the cross-linked BDDE molecule. These results are very similar to those of a previous study (Zhang et al., 2014). The results of the FT-IR spectra assay proved that HA successfully cross-linked with BC in the presence of BDDE.

#### 3.1.2. Morphology of BC and BC/HA composites

The fabricated BC and BC/HA composites were freeze-dried, and their surface morphological characteristics were observed by FE-SEM as presented in Figs. 3 and S1. Surface images show that freeze-dried BC exhibits a 3-D network of nanofibrils in the form of a heterogeneous porous structure (Fig. 3A) which agrees with the typical morphology reported for BC (Dayal & Catchmark, 2016). This highly developed pore size is not conducive to cell proliferation, differentiation and adhesion

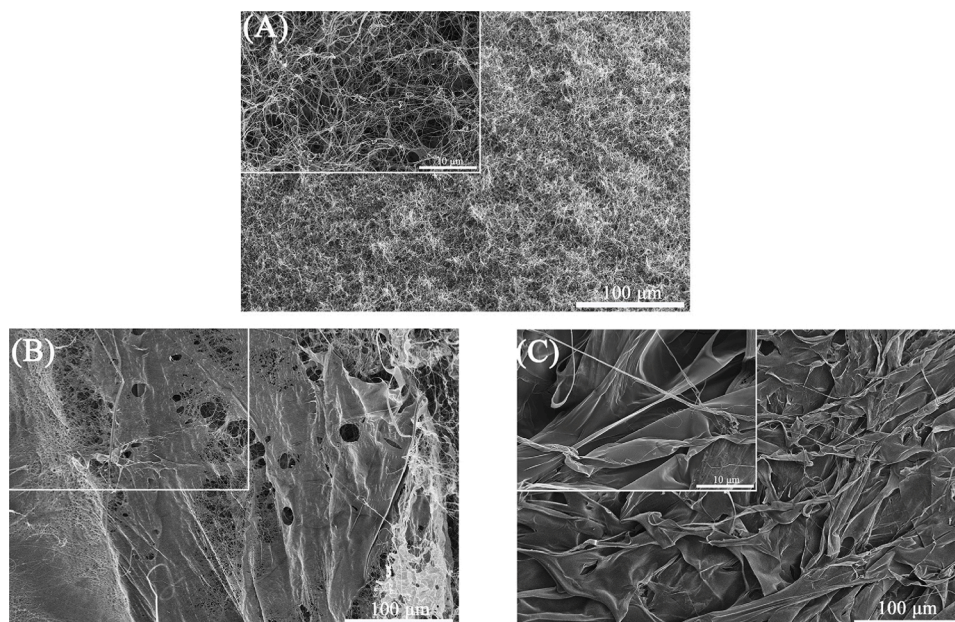


Fig. 3. FE-SEM surface images of (A) pure BC, (B) BC/HA<sub>2-0</sub> and (C) BC/HA<sub>2-1</sub> with magnifications of 1000 and 10 000 times (inset).

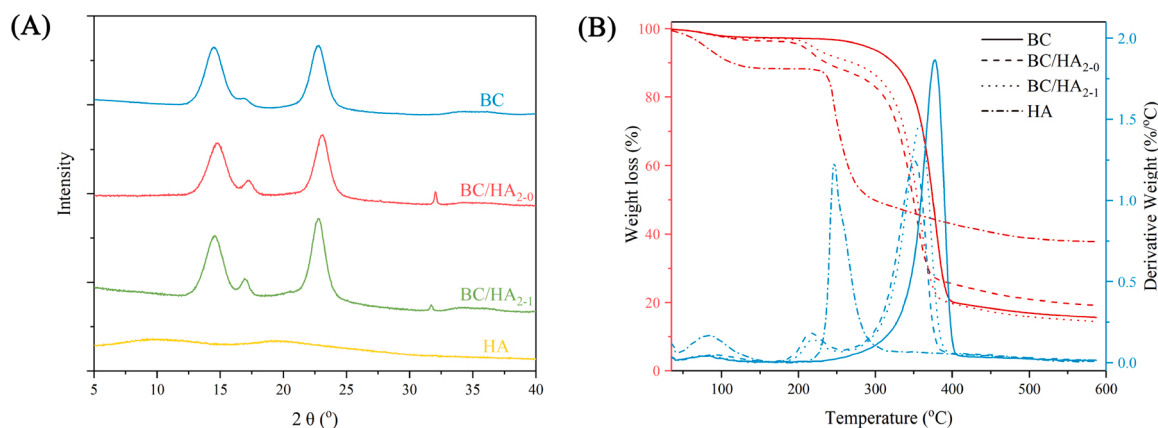


Fig. 4. (A) XRD curves of BC, HA and BC/HA composites, (B) TG and DTG curves of BC, HA and BC/HA composites.

(Sanchavanakit et al., 2006). The surface structure of the BC film was changed by adding HA. The BC/HA composite without crosslinking was completely different from the pure BC surface, showing a relatively smooth surface. HA tends to associate with BC and bundle BC fibers as shown in Figs. S1A and S1B. As the concentration increases, HA covers the entire fiber layer, forming a relatively flat surface. However, because HA itself is water-soluble, it will be slowly released into the solution and form uneven holes (Fig. 3B), reducing the useful life of the material. When BDDE is present, the surface of the material changed dramatically. The crosslinking of the material via BDDE process has produced a denser surface. When the HA concentration was 0.5 %, more fibers were wrapped into a thicker bundle by the cross-linked HA. When the concentration was increased to 2%, it was difficult to find BC fibers. The surface of the BC film has been completely covered by cross-linked HA, forming a dense structure (Fig. 3C). Therefore, the stability of BC/HA composites can be achieved by chemical crosslinking. Pure HA crosslinking has also been reported for tissue filling (Yang, Tan, Cen, & Zhang, 2016). HA is highly hydrophilic, which can increase cell migration during wound healing and promote wound healing (Cheng et al., 2013). In summary, BC/HA composites formed by cross-linking agents may have several advantages over pure BC in many current and future medical applications.

### 3.1.3. XRD analysis

The XRD patterns of BC, HA, and BC/HA composites are shown in Fig. 4A. Both BC and BC/HA composites displayed three major crystallographic planes  $\langle 100 \rangle$ ,  $\langle 010 \rangle$ , and  $\langle 110 \rangle$  at  $2\theta$  angles of around  $14.7^\circ$ ,  $17.2^\circ$ , and  $22.8^\circ$ , respectively. The higher intensity of the peak at  $2\theta = 14.7^\circ$  than that of the peak at  $2\theta = 17.2^\circ$  indicated the predominant cellulose I $\alpha$  allomorph (one-chain triclinic crystal structure) characteristic of cellulose produced by *G. hansenii*. These results were in agreement with our previous studies (Chi & Catchmark, 2017; Liu & Catchmark, 2019b). For HA, no obvious peak was observed on its XRD pattern, suggesting that it is amorphous. The CrI and crystal size of three major crystallographic planes were summarized in Table S1, and there was no significant difference for BC and BC/HA composites, implying that the crystallization and co-crystallization of cellulose microfibrils were not impacted. In our previous study (Chi & Catchmark, 2017), different additives (such as xyloglucan, xylan, exopolysaccharides, etc.) were incorporated into BC through an in-situ approach, i.e. adding material into the culture medium during BC biosynthesis and showed different interfering roles, resulting in changes in CrI, crystalline dimensions and allomorph content (cellulose I $\alpha$ /I $\beta$  ratio). These additives could either interact with cellulose fibrils via hydrogen bonding and van der Waals interactions during BC crystallization or co-crystallization process (in the case of xylan and xyloglucan) or disrupt the physical aggregation process of BC (in the case of exopolysaccharides) (Chi & Catchmark, 2017). In another study, BC/HA composites were produced

by co-culturing *G. hansenii* and *Lactococcus lactis* APJ13, which was essentially an in-situ modification of BC (Liu & Catchmark, 2019b). The XRD data suggested that the presence of HA was unable to impact the CrI of cellulose but increased the crystalline dimensions in  $\langle 100 \rangle$  and  $\langle 010 \rangle$  planes, suggesting HA aided in co-crystallization of BC. Herein, HA was incorporated into the BC network using an ex-situ process, which was unable to interfere with the BC biosynthesis process as evidenced by the similar CrI and crystalline dimension data (Table S1). Interestingly, a peak was observed at  $2\theta = 31.8^\circ$  for BC/HA $_{2-0}$  and BC/HA $_{2-1}$  composite, and this peak was more obvious in BC/HA $_{2-0}$ . This peak was unidentified but may arise from the co-crystallization or some ordering associated with the interaction between the BC and HA. After addition of BDDE, the crosslinking role of BDDE may interfere with the hydrogen-bonding induced co-crystallization between BC and HA.

### 3.1.4. Thermal stability

The thermal stability of BC/HA composites is another important parameter considering its potential biomedical applications, which would require antiseptic treatment at high temperature. Fig. 4B showed the TG and DTG curves of BC, HA, and BC/HA composites at the temperature range from 35 to 600 °C. All samples displayed an initial weight loss between 35 and 100 °C due to the evaporation of absorbed moisture. A higher weight loss was found for HA at this temperature range, which might be caused by its higher water sorption ability from the environment. At the temperature range from 100 to 500 °C, the native BC sample showed typical one-step thermal degradation with the maximum degradation temperature ( $T_{max}$ ) at 378 °C. For HA, the one-step thermal decomposition was also observed with  $T_{max}$  (246 °C) much lower than that of BC, possibly ascribed to its amorphous nature as seen from XRD data. It has been reported that thermal stability is impacted by several physical and chemical factors including crystalline structure, surface chemistry, degree of polymerization (Chi & Catchmark, 2017). We speculate crystallinity, surface chemistry (functional groups and charge density), and degree of polymerization (DP) are the most important and relevant parameters for thermal stability analysis of BC/HA composites in the current study. For example, BC and HA are different in crystallinity (83 % vs. 0%), surface chemistry (OH groups vs. COOH/OH groups), and DP (8000–12000 vs. 3000–4000). These major structural and chemical differences and their interplay have caused the observed thermal stability difference (e.g. maximum thermal degradation temperature) for BC and HA, as indicated in TGA curves. In the case of BC/HA composites, two thermal degradation peaks were found on the DTG curves at  $\sim 215^\circ\text{C}$  and between 300–400 °C. The decomposition at 215 °C could be related to the surface coated, freely associated HA, while a higher degradation temperature (350 °C for BC/HA $_{2-0}$  and 360 °C for BC/HA $_{2-1}$ ) might result from the intimately associated BC/HA network. It is also indicative that BDDE-induced crosslinking could improve the  $T_{max}$  of the resulting composites.

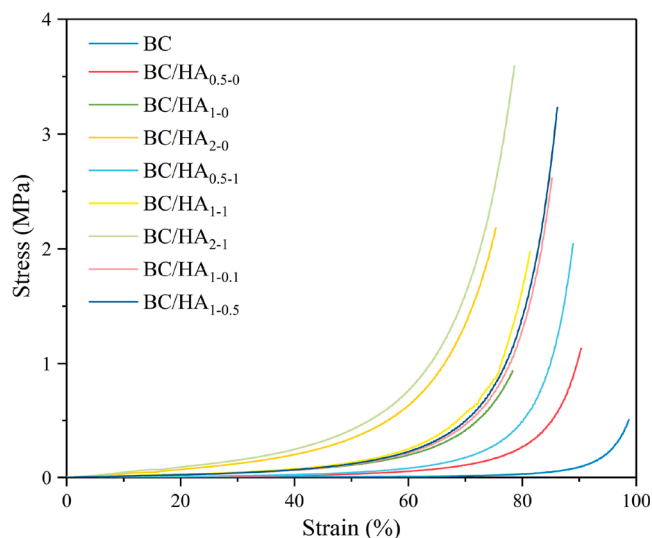


Fig. 5. Compressive stress-strain curves of BC and BC/HA composites.

### 3.1.5. Mechanical properties

The effect of HA and crosslinkers on the compression properties of BC composites is presented in Table 2. Fig. 5 shows typical compressive stress-strain curves for BC and BC/HA composites. In the initial stage of compression, the change of stress is not obvious with the increase of strain, especially for the original BC. As the load increases, the stress increases sharply. During compression, when pressed in a direction perpendicular to the stratified structure of BC, water is forced out of the BC samples. For BC/HA composites without crosslinking, this situation is relatively complex, because HA itself has strong water retention capacity and extremely high viscosity. BC is a multi-layer structure with a layer distance of about 5  $\mu\text{m}$  between layers, making it difficult to form hydrogen bonds (Henning & Catchmark, 2017; Suryanto, Muhajir, Sutrisno, Zakia, & Yanuhar, 2019). So, another key issue is that HA fills

the network voids within BC and forms high-density hydrogen bonds with BC. In this case, HA and water are difficult to squeeze out from the BC, which greatly increases the compression resistance of the material. This result is consistent with other BC composite materials (Dayal & Catchmark, 2016). By chemically crosslinking with BDDE, the compressive modulus and compressive stress of the material are further enhanced. As the concentration of the cross-linking agent increases, a modest increase in compressive modulus and compressive stress is observed (Table S2). This indicates that the stability of HA in BC is further enhanced by cross-linking, which hinders the expulsion of HA and water under compressive stress. As shown by the FE-SEM (Fig. 3G), a high-density, low-void surface structure was formed. At the same time, HA will be cross-linked with BC through BDDE, and this part of HA cannot be squeezed out of BC. Therefore, HA and BDDE increase the compression modulus of the material, which is directly related to the binding affinity of the filler and BC and their own water holding capacity.

Many biomedical materials also require specific tensile behavior. The typical stress-strain curves, tensile strength, Young's modulus and strain at break of the samples tested are shown in Fig. 6. Pure BC showed the highest tensile strength and Young's modulus. The addition of HA reduces the overall strength of the material. With the increase in HA concentration, the strength of the material further decreases. When the concentration increases from 0.5% to 2%, the tensile strength decreases from 0.73 MPa to 0.54 MPa, and the Young's modulus decreases from 1.74 MPa to 1.25 MPa. The breaking point elongation (breaking strain) of the HA composite film is higher than that of pure BC, showing an increasing trend with increasing HA concentration. As shown by XRD (Fig. 4A), HA itself is amorphous and lacks mechanical strength. It has been reported that blending generally amorphous materials with higher mechanical strength materials often results in a reduction in the overall mechanical strength of the composite material (Chiaooprakobkij et al., 2011; Li et al., 2015; Wu et al., 2004). This phenomenon may be related to changes in the hydrogen bonding of the composite material. The participation of HA formed new hydrogen bonds and reduced the strong hydrogen bonds between the original BC fibers. The tensile test is

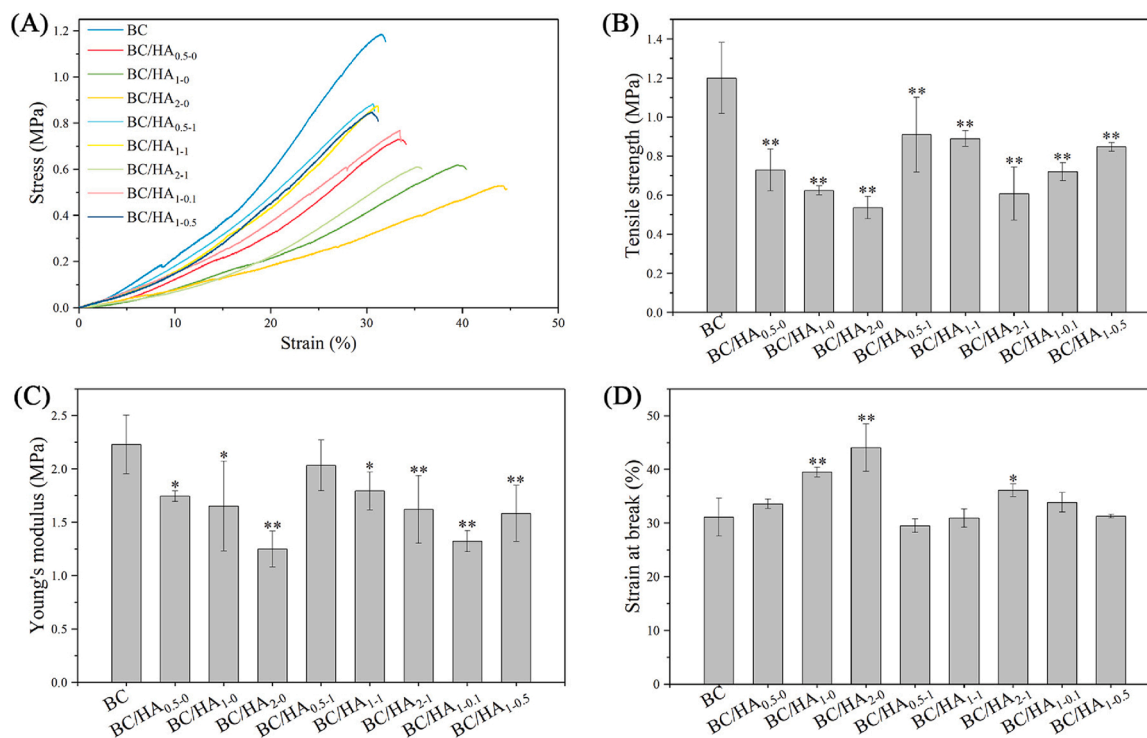
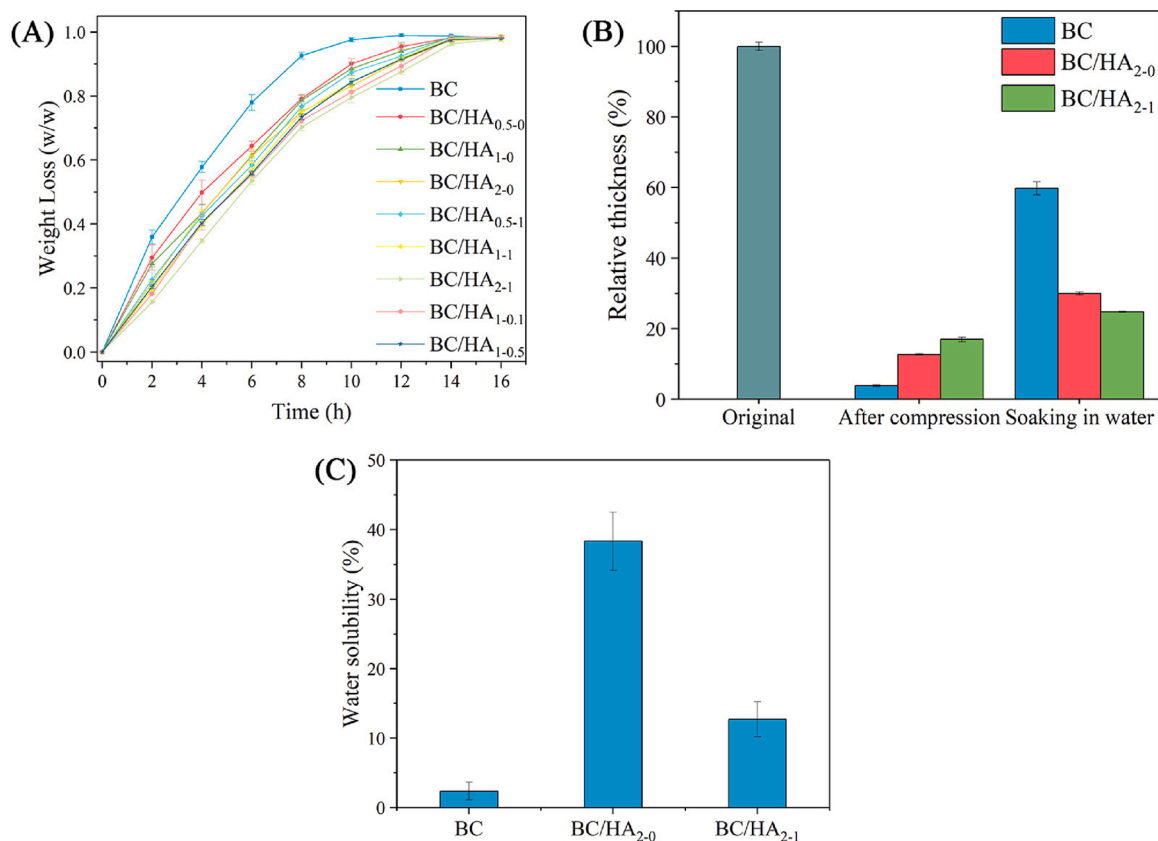


Fig. 6. Tensile properties of wet BC and BC/HA composites. (A) typical stress-strain curves, (B) tensile strength, (C) Young's modulus, and (D) strain at break. \*  $p < 0.05$ ; \*\*  $p < 0.01$ .



**Fig. 7.** (A) Water loss from BC and BC/HA composites as a function of time, (B) Recovery of compressed BC and BC/HA composites in water, and (C) Water solubility test of BC and BC/HA composites.

different from the compression test and involves the breaking strength of the flat layers that comprise the BC pellicle. To improve this lack of strength of composite material, BDDE is used to crosslink macromolecular chains. The BDDE cross-links HA and HA, HA and BC or BC and BC fibers together, which improves the material's resistance to fracture. The elongation at the breaking point of the composite was significantly increased in the presence of HA, and was positively correlated with the HA concentration. When HA concentration is 2%, the elongation at the break point of the BDDE cross-linked BC/HA composite is higher than that of pure BC, but lower than that of the uncross-linked BC/HA composite with the same HA concentration. This may result from increased rigidity of the composite material from additional BC-BC/BC-HA/BC-HA-BC bonds formed via crosslinking, which are stronger and more numerous than in non-cross-linked BC/HA composites, but less numerous than BC-BC bonds in pure BC. Due to its excellent mechanical strength, BC has been used as a wound dressing and skin repair material (Czaja et al., 2007; Li, Kim, Lee, Kee, & Oh, 2011). In summary, the addition of BDDE makes up for the loss of strength caused by HA addition.

### 3.2. Water retention property, water absorptivity and water solubility

Water content and water holding capacity are important indicators of biological materials (Xu et al., 2016). The fibers of BC are stacked alternately to form a highly porous structure. This structure allows BC to have high-water content (more than 99%), which makes it widely used as a wound dressing biomaterial (Ul-Islam, Shah, Ha, & Park, 2011). However, well-developed voids will accelerate the release of moisture. Therefore, BC composite membranes can often be prepared to reduce water release. As shown in Fig. 7A, the addition of HA greatly reduced weight loss. With the increase of HA content, the water loss rate decreases. This is possible because HA itself has good water absorption and

water retention capabilities. At the same time, HA will fill the voids in BC to reduce the emission of moisture. Interestingly, the cross-linking of BDDE further alleviates the loss of water. This may be due to the better coverage of the BC film by the cross-linked HA, as shown by FE-SEM (Fig. 3), forming a dense surface layer. In summary, the cross-linked BC/HA composite can reduce the loss of water in wound care applications, keeping the wound moist for a longer time, which would improve wound healing.

The material's water absorption capacity and structural stability may play an important role in its practical use in biomedical applications. Resilience was examined by compressing a sample, and then observing its dimensional recovery in water. As shown in Fig. 7B, different samples exhibit different degrees of deformation after exposure to compressive stress, which is consistent with the mechanical strength test. When the sample was immersed in water again, the pure BC recovered from 3.0% after compression to 59.8%. BC/HA<sub>2-0</sub> rebound is relatively difficult, only recovering from 12.7% after compression to 30.0%. After BDDE cross-linking, recovery is also poor, returning from a compression of 16.9%–24.8%. Pure BC may recover well because the large voids can quickly absorb water and swell. The presence of HA leads to a reduction in the amount of BC pores, and BDDE cross-linking further results in denser HA coverage. The unique physical and chemical structure formed between HA and BC will also affect the stretch of BC fibers (Oliveira Barud et al., 2015). The swelling capacity of the material can be adjusted by HA, which may be of interest in the treatment of wounds with different levels of exudation.

The stability of the material is also an important parameter, especially considering its biological applications. Due to the inherent hydrophilicity and water solubility, HA is readily dissolved in aqueous solution. On the other hand, the highly ordered crystallites packing and high crystallinity has made BC completely insoluble in water. As shown in Fig. 7C, the solubility of the uncross-linked BC/HA composite is as

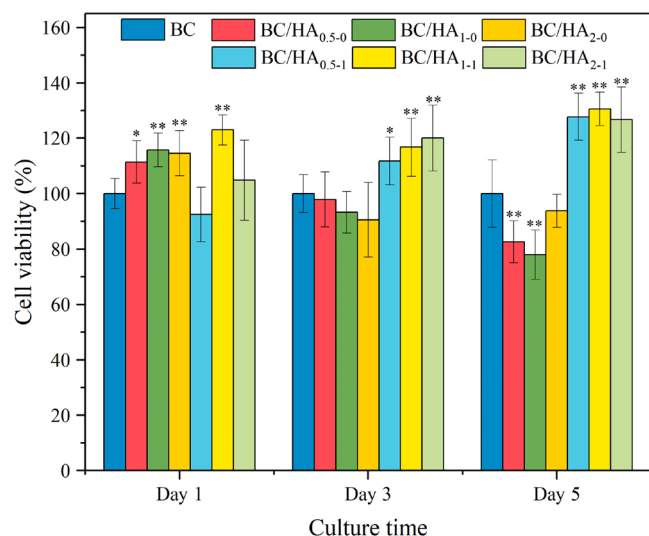


**Fig. 8.** Percentage of cell viability by CCK-8 assay in L929 cells after coculture with the BC and BC/HA composite films in 1, 3 and 5 days ( $n = 6$ ). \* $p < 0.05$  and \*\* $p < 0.01$  compared with original BC group.

high as 38.34 %, which mainly arises from the solubility and release of HA from the BC fiber network. However, after BDDE cross-linking, the water solubility of the composite is largely reduced, measuring only 12.72 %, implying that the chemical crosslinking bridged by BDDE has significantly restricted the polymer chain mobility of HA even when HA will partially degrade under alkaline conditions. This reduced water solubility shows that the cross-linked BC/HA composite has better stability and is more suitable for practical applications.

### 3.3. Cell evaluation

BDDE cross-linked HA has been proven to be safe for tissue engineering and dermal fillers (Baek et al., 2018; Yang et al., 2016). In the present study, the cell viability of BC and BC/HA composites created were tested using L929 cells after 1, 3, and 5 days. Previous studies have confirmed that BC has no cytotoxic effect on a variety of cells (Czaja, Krystynowicz, Bielecki, & Brown, 2006; Svensson et al., 2005). The result of the CCK-8 assay is presented in Fig. 8. Compared with the original BC, the BC/HA composite does not inhibit cell growth. The BC/HA composite without crosslinking shows similar cellular activity to the original BC. On the first day of culture, the cell viability was slightly higher than the original BC. With the increase of culture time, although the cell viability was reduced, it still maintained 90 % activity relative to the original BC. This may be because the cells have grown to the inside of the material, and not all cells were isolated during the measurement. When BDDE is involved in cross-linking, the BC/HA composites shows superior ability to promote cell growth. With the increase of the culture time, this advantage becomes more obvious, and the cell viability increased by up to 30.1 % when cultured for 5 days. This result may be attributed to the surface flatness of the material (Washburn, Weir, Anderson, & Potter, 2004). According to the FE-SEM results (Fig. 3), the BDDE cross-linked BC/HA composites exhibit a rough surface structure. A certain roughness can increase the surface area of cell adhesion and promote cell adhesion, growth, and proliferation (Rosales-Leal et al., 2010). These results indicate that the BDDE-cross-linked BC/HA composites not only maintain a high degree of biocompatibility, but also enhance the proliferation of the cells. The composite material may release part of the HA, and HA plays a positive role in enhancing mitochondrial repair capacity and cell viability (Grishko et al., 2009).

Cell viability assays of BC/HA composites were visually validated using live/dead staining of L929 cells via fluorescence microscopy and compared to native BC (Fig. 9A). After five-day cultivation, the surface

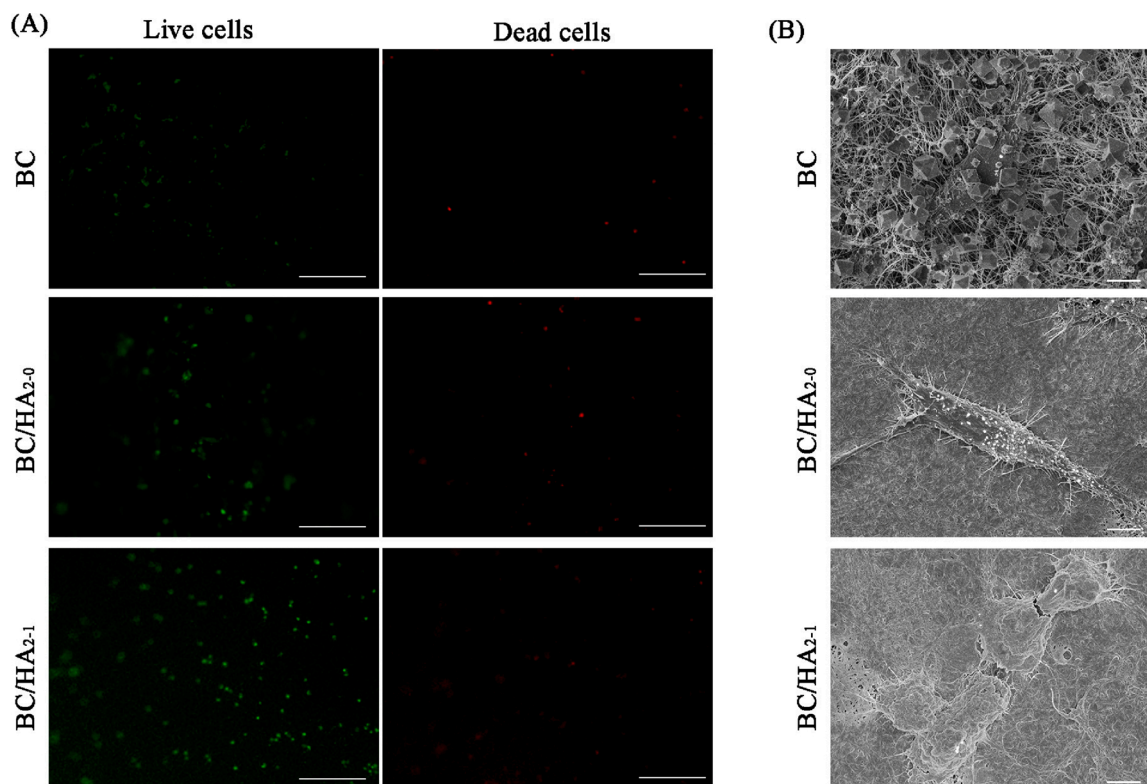


**Fig. 9.** (A) Fluorescence microscopy images of calcein AM/EthD-1 stained L929 cells after five-day culture on the surface of BC and BC/HA composite films (scale bar, 200  $\mu\text{m}$ ). Live cells were stained green and dead cells were stained red. (B) L929 cells adhesion morphology on the surface of BC and BC/HA composite films after five-day cultivation (scale bar, 5  $\mu\text{m}$ ) (For interpretation of the references to colour in this figure legend, the reader is referred to the web version of this article).

of all samples exhibited green fluorescence, indicating that the cells have good viability on the surface of BC-based material. A further analysis indicates a preferable viability of L929 cells in cross-linked BC/HA composites, as indicated by the increased number of live cells on the surface. We hypothesize that this preferable viability may be due to the increased surface density and texture of BDDE crosslinked BC/HA composites, implying that a denser and smoother surface covered by HA may facilitate cells to grow.

We further characterized the adhesion of L929 cells on BC and BC/HA composite by SEM imaging (Fig. 9B). The porous network of native BC fibers can direct cell growth to the surface. However, the porous network may not be conducive to cell adhesion. In contrast, the cells on the surface of BC/HA composites had many pseudopodia and formed a layer on the surface. These results indicated that the cells stretched their morphology and were proliferating, possibly due to the formation of a flatter or denser surface area that improve the cell attachment. The growing cells on the cross-linked BC/HA composite demonstrated a morphology closer to the surface, achieving a better scattering attachment on BC/HA specimen. Thus, cell morphology study suggests that formation of a more even or denser surface area in crosslinked BC/HA composite results in a different surface structure, such as porosity or stiffness, to improve cell attachment. Combining with its superior mechanical strength, the cross-linked BC/HA composite may be useful as a wound dressing material.

#### 4. Conclusions

A series of bacterial cellulose/hyaluronic acid (BC/HA) composites were obtained by varying concentrations of HA and crosslinking agent (1,4-butanediol diglycidyl ether, BDDE). Through crosslinking, a smooth and dense HA surface layer was successfully formed on the surface of BC. The BDDE cross-linked BC/HA composite has better water retention capacity, lower deformation and water solubility than uncross-linked BC/HA. The improved compression modulus may improve the ability of BC to protect the wound from external friction or impact injury. *in vitro* experiments on mouse fibroblast cells indicated that the BDDE cross-linked BC/HA composites enhanced cell proliferation and attachment as compared to pure BC. In summary, improved mechanical properties and better cell compatibility make BC/HA composite hydrogels a good candidate for skin repair wound dressings. Further work is needed to understand the practical applications of these composites.

#### CRedit authorship contribution statement

**Shuo Tang:** Conceptualization, Methodology, Validation, Data curation, Writing - original draft. **Kai Chi:** Validation, Data curation, Writing - original draft. **Hui Xu:** Validation, Data curation. **Qiang Yong:** Supervision, Funding acquisition. **Jian Yang:** Supervision, Resources. **Jeffrey M. Catchmark:** Resources, Supervision, Writing - review & editing, Project administration, Funding acquisition.

#### Acknowledgments

This work was supported by the National Key R&D Program of China (2016YFD0600803), State Key Laboratory of Pulp and Paper Engineering (201812) and the USDA National Institute of Food and Agriculture Federal Appropriations under Project PAES 4602 (1009850). The authors thank the Project of First-Class Discipline and the Doctorate Fellowship of Nanjing Forestry University for supporting the work presented in this paper.

#### Appendix A. Supplementary data

Supplementary material related to this article can be found, in the online version, at doi:<https://doi.org/10.1016/j.carbpol.2020.117123>.

#### References

- Baek, J., Fan, Y., Jeong, S. H., Lee, H. Y., Jung, H. D., Kim, H. E., et al. (2018). Facile strategy involving low-temperature chemical cross-linking to enhance the physical and biological properties of hyaluronic acid hydrogel. *Carbohydrate Polymers*, 202, 545–553.
- Carvalho, T., Guedes, G., Sousa, F. L., Freire, C. S. R., & Santos, H. A. (2019). Latest advances on bacterial cellulose-based materials for wound healing, delivery systems, and tissue engineering. *Biotechnology Journal*, 14(12), Article 1900059.
- Cen, L., Neoh, K. G., Li, & Kang, E. T. (2004). Assessment of *in vitro* bioactivity of hyaluronic acid and sulfated hyaluronic acid functionalized electroactive polymer. *Biomacromolecules*, 5(6), 2238–2246.
- Cheng, L., Sun, X., Li, B., Hu, C., Yang, H., Zhang, Y., et al. (2013). Electrospun Ginsenoside Rg3/poly(lactic-co-glycolic acid) fibers coated with hyaluronic acid for repairing and inhibiting hypertrophic scars. *Journal of Materials Chemistry B*, 1(35), 4428–4437.
- Chi, K., & Catchmark, J. M. (2017). The influences of added polysaccharides on the properties of bacterial crystalline nanocellulose. *Nanoscale*, 9(39), 15144–15158.
- Chiaoprakobkij, N., Sanchavanakit, N., Subbalekha, K., Pavasant, P., & Phisalaphong, M. (2011). Characterization and biocompatibility of bacterial cellulose/alginate composite sponges with human keratinocytes and gingival fibroblasts. *Carbohydrate Polymers*, 85(3), 548–553.
- Czaja, W., Krystynowicz, A., Bielecki, S., & Brown, R. M. (2006). Microbial cellulose—the natural power to heal wounds. *Biomaterials*, 27(2), 145–151.
- Czaja, W. K., Young, D. J., Kawecky, M., & Brown, R. M. (2007). The future prospects of microbial cellulose in biomedical applications. *Biomacromolecules*, 8(1), 1–12.
- Dayal, M. S., & Catchmark, J. M. (2016). Mechanical and structural property analysis of bacterial cellulose composites. *Carbohydrate Polymers*, 144, 447–453.
- De Boule, K., Glogau, R., Kono, T., Nathan, M., Tezel, A., Roca-Martinez, J. X., et al. (2013). A review of the metabolism of 1,4-Butanediol diglycidyl ether-cross-linked hyaluronic acid dermal fillers. *Dermatologic Surgery*, 39(12), 1758–1766.
- de Oliveira, S. A., da Silva, B. C., Riegel-Vidotti, I. C., Urbano, A., de Sousa Faria-Tischer, P. C., & Tischer, C. A. (2017). Production and characterization of bacterial cellulose membranes with hyaluronic acid from chicken comb. *International Journal of Biological Macromolecules*, 97, 642–653.
- Dong, H., Zheng, L., Yu, P., Jiang, Q., Wu, Y., Huang, C., et al. (2020). Characterization and application of lignin-carbohydrate complexes from lignocellulosic materials as antioxidants for scavenging *in vitro* and *in vivo* reactive oxygen species. *ACS Sustainable Chemistry & Engineering*, 8(1), 256–266.
- Grishko, V., Xu, M., Ho, R., Mates, A., Watson, S., Kim, J. T., et al. (2009). Effects of hyaluronic acid on mitochondrial function and mitochondria-driven apoptosis following oxidative stress in human chondrocytes. *The Journal of Biological Chemistry*, 284(14), 9132–9139.
- Henning, A. L., & Catchmark, J. M. (2017). The impact of antibiotics on bacterial cellulose *in vivo*. *Cellulose*, 24(3), 1261–1285.
- Jeon, O., Song, S. J., Lee, K. J., Park, M. H., Lee, S. H., Hahn, S. K., et al. (2007). Mechanical properties and degradation behaviors of hyaluronic acid hydrogels cross-linked at various cross-linking densities. *Carbohydrate Polymers*, 70(3), 251–257.
- Jia, Y., Huo, M., Huang, H., Fu, W., Wang, Y., Zhang, J., et al. (2015). Preparation and characterization of bacterial cellulose/hyaluronic acid composites. *Proceedings of the Institution of Mechanical Engineers Part N Journal of Nanoengineering and Nanosystems*, 229(1), 41–48.
- Lamboni, L., Li, Y., Liu, J., & Yang, G. (2016). Silk sericin-functionalized bacterial cellulose as a potential wound-healing biomaterial. *Biomacromolecules*, 17(9), 3076–3084.
- Li, H. X., Kim, S., Lee, Y., Kee, C., Oh, K., et al. (2011). Determination of the stoichiometry and critical oxygen tension in the production culture of bacterial cellulose using saccharified food wastes. *The Korean Journal of Chemical Engineering*, 28, 2306–2311.
- Li, Y., Jiang, H., Zheng, W., Gong, N., Chen, L., Jiang, X., et al. (2015). Bacterial cellulose-hyaluronan nanocomposite biomaterials as wound dressings for severe skin injury repair. *Journal of Materials Chemistry B*, 3(17), 3498–3507.
- Li, Y., Qing, S., Zhou, J., & Yang, G. (2014). Evaluation of bacterial cellulose/hyaluronan nanocomposite biomaterials. *Carbohydrate Polymers*, 103, 496–501.
- Lin, W. C., Lien, C. C., Yeh, H. J., Yu, C. M., & Hsu, S. (2013). Bacterial cellulose and bacterial cellulose-chitosan membranes for wound dressing applications. *Carbohydrate Polymers*, 94(1), 603–611.
- Liu, K., & Catchmark, J. M. (2019a). Enhanced mechanical properties of bacterial cellulose nanocomposites produced by co-culturing *Gluconacetobacter hansenii* and *Escherichia coli* under static conditions. *Carbohydrate Polymers*, 219, 12–20.
- Liu, K., & Catchmark, J. M. (2019b). Bacterial cellulose/hyaluronic acid nanocomposites production through co-culturing *Gluconacetobacter hansenii* and *Lactococcus lactis* in a two-vessel circulating system. *Bioresource Technology*, 290, Article 121715.
- Nakayama, A., Kakugo, A., Gong, J. P., Osada, Y., Takai, M., Erata, T., et al. (2004). High mechanical strength double-network hydrogel with bacterial cellulose. *Advanced Functional Materials*, 14(11), 1124–1128.
- Necas, J., Bartosikova, L., Brauner, P., & Kolar, J. (2008). Hyaluronic acid (hyaluronan): A review. *Veterinari Medicina*, 53(8), 397–411.
- Oliveira Barud, H. G., Barud, H. d. S., Cavicchioli, M., do Amaral, T. S., Junior, O. B. d. O., Santos, D. M., et al. (2015). Preparation and characterization of a bacterial cellulose/silk fibroin sponge scaffold for tissue regeneration. *Carbohydrate Polymers*, 128, 41–51.
- Pitarresi, G., Palumbo, F. S., Tripodo, G., Cavallaro, G., & Giammona, G. (2007). Preparation and characterization of new hydrogels based on hyaluronic acid and  $\alpha,\beta$ -polyaspartylhydrazide. *European Polymer Journal*, 43(9), 3953–3962.

- Prosdoci, M., & Bevilacqua, C. (2012). Exogenous hyaluronic acid and wound healing: An updated vision. *Panminerva Medica*, 54(2), 129–135.
- Ramachandran, B., Chakraborty, S., Kannan, R., Dixit, M., & Muthuvijayan, V. (2019). Immobilization of hyaluronic acid from *Lactococcus lactis* on polyethylene terephthalate for improved biocompatibility and drug release. *Carbohydrate Polymers*, 206, 132–140.
- Rosales-Leal, J. I., Rodríguez-Valverde, M. A., Mazzaglia, G., Ramón-Torregrosa, P. J., Díaz-Rodríguez, L., García-Martínez, O., et al. (2010). Effect of roughness, wettability and morphology of engineered titanium surfaces on osteoblast-like cell adhesion. *Colloids and Surfaces A, Physicochemical and Engineering Aspects*, 365(1–3), 222–229.
- Sanchavanakit, N., Sangrungrangroj, W., Kaomongkolgit, R., Banaprasert, T., Pavasant, P., & Phisalaphong, M. (2006). Growth of human keratinocytes and fibroblasts on bacterial cellulose film. *Biotechnology Progress*, 22(4), 1194–1199.
- Shah, N., Ul-Islam, M., Khattak, W. A., & Park, J. K. (2013). Overview of bacterial cellulose composites: A multipurpose advanced material. *Carbohydrate Polymers*, 98(2), 1585–1598.
- Suryanto, H., Muhajir, M., Sutrisno, T., Zakia, N., & Yanuhar, U. (2019). The mechanical strength and morphology of bacterial cellulose films: The effect of NaOH concentration. *IOP Conference Series: Materials Science and Engineering*, 515, Article 012053. IOP Publishing.
- Svensson, A., Nicklasson, E., Harrah, T., Panilaitis, B., Kaplan, D. L., Brittberg, M., et al. (2005). Bacterial cellulose as a potential scaffold for tissue engineering of cartilage. *Biomaterials*, 26(4), 419–431.
- Treesuppharat, W., Rojanapanthu, P., Siangsano, C., Manuspiya, H., & Ummartyotin, S. (2017). Synthesis and characterization of bacterial cellulose and gelatin-based hydrogel composites for drug-delivery systems. *Biotechnology Reports*, 15, 84–91.
- Ul-Islam, M., Shah, N., Ha, J. H., & Park, J. K. (2011). Effect of chitosan penetration on physico-chemical and mechanical properties of bacterial cellulose. *The Korean Journal of Chemical Engineering*, 28(8), 1736.
- Wang, J., Wan, Y. Z., Luo, H. L., Gao, C., & Huang, Y. (2012). Immobilization of gelatin on bacterial cellulose nanofibers surface via crosslinking technique. *Materials Science and Engineering C*, 32(3), 536–541.
- Washburn, N. R., Weir, M., Anderson, P., & Potter, K. (2004). Bone formation in polymeric scaffolds evaluated by proton magnetic resonance microscopy and X-ray microtomography. *Journal of Biomedical Materials Research Part A: An Official Journal of The Society for Biomaterials, The Japanese Society for Biomaterials, and The Australian Society for Biomaterials and the Korean Society for Biomaterials*, 69(4), 738–747.
- Weissmann, B., & Meyer, K. (1954). The structure of hyalobiuronic acid and of hyaluronic acid from umbilical Cord1, 2. *Journal of the American Chemical Society*, 76(7), 1753–1757.
- Wu, Y.-B., Yu, S.-H., Mi, F.-L., Wu, C.-W., Shyu, S.-S., Peng, C.-K., et al. (2004). Preparation and characterization on mechanical and antibacterial properties of chitsoan/cellulose blends. *Carbohydrate Polymers*, 57(4), 435–440.
- Xu, R., Xia, H., He, W., Li, Z., Zhao, J., Liu, B., et al. (2016). Controlled water vapor transmission rate promotes wound-healing via wound re-epithelialization and contraction enhancement. *Scientific Reports*, 6(1), 24596.
- Yang, R., Tan, L., Cen, L., & Zhang, Z. (2016). An injectable scaffold based on cross-linked hyaluronic acid gel for tissue regeneration. *RSC Advances*, 6(20), 16838–16850.
- Zhang, J., Ma, X., Fan, D., Zhu, C., Deng, J., Hui, J., et al. (2014). Synthesis and characterization of hyaluronic acid/human-like collagen hydrogels. *Materials Science and Engineering C*, 43, 547–554.